

Analysis of simulated data for the Karlsruhe TRItium Neutrino experiment using Bayesian inference

Anna Sejersen Riis

Department of Physics and Astronomy, University of Aarhus, Ny Munkegade, DK-8000 Aarhus C, Denmark and Institute of Nuclear Physics, Westfälische Wilhelms-Universität, Wilhelm-Klemm-Strasse 9, D-48149 Münster, Germany

Steen Hannestad

Department of Physics and Astronomy, University of Aarhus, Ny Munkegade, DK-8000 Aarhus C, Denmark

Christian Weinheimer

Institute of Nuclear Physics, Westfälische Wilhelms-Universität, Wilhelm-Klemm-Strasse 9, D-48149 Münster, Germany

(Received 31 May 2011; published 31 October 2011)

The KATRIN (Karlsruhe Tritium Neutrino) experiment will analyze the tritium β spectrum to determine the mass of the neutrino with a sensitivity of 0.2 eV (90% C.L.). This approach to a measurement of the absolute value of the neutrino mass relies only on the principle of energy conservation and can in some sense be called model-independent as compared to cosmology and neutrinoless double β decay. However, by model independent we only mean in case of the minimal extension of the standard model. One should therefore also analyze the data for nonstandard couplings to, e.g., right-handed or sterile neutrinos. As an alternative to the frequentist minimization methods used in the analysis of the earlier experiments in Mainz and Troitsk we have been investigating Markov chain Monte Carlo (MCMC) methods which are very well suited for probing multiparameter spaces. We found that implementing the KATRIN χ^2 function in the COSMOMC package—an MCMC code using Bayesian parameter inference—solved the task at hand very nicely.

DOI: [10.1103/PhysRevC.84.045503](https://doi.org/10.1103/PhysRevC.84.045503)

PACS number(s): 29.85.Fj, 23.40.Bw, 14.60.St

I. INTRODUCTION

The Karlsruhe Tritium Neutrino experiment, KATRIN [1,2], is a β -decay experiment attempting to measure the electron neutrino mass with subelectronvolt precision. Presently the experiment is commissioned to start data-taking in 2013-2014 and has a projected sensitivity of 0.2 eV (90% C.L.) to the neutrino mass.

KATRIN is the successor of the experiments in Mainz [3] and Troitsk [4] and we will be using some of the same techniques as those. For additional technical details about KATRIN, see, e.g., [1,2,5].

Strictly speaking, when measuring the “electron” neutrino mass with β -decay spectra, what we get is the so-called kinematic neutrino mass. That is, the incoherent sum of neutrino mass eigenvalues weighted by the appropriate entries in the lepton mixing matrix:

$$m_{\nu_e}^2 = \sum_{i=0}^n |U_{ei}|^2 m_i^2. \quad (1)$$

However, because the mass differences between the active neutrino mass states are known to be smaller than KATRIN’s sensitivity, the experiment can effectively only see one mass state (the mass-squared differences are $\Delta m_{12}^2 = 8 \times 10^{-5} \text{ eV}^2$ and $\Delta m_{23}^2 = |2.6 \times 10^{-3}| \text{ eV}^2$, respectively [6]). This mass state is sometimes called the “electron” neutrino mass, but in principle the tritium β spectrum could contain the signatures of more than one mass state or of couplings to other particles entirely. In order to be called truly model independent, KATRIN’s final data should be analyzed also for alternative scenarios beyond the minimal extension of the standard model.

Performing an analysis for nonstandard couplings to the electron neutrino adds more parameter space to the χ^2 function of the experiment. One should therefore consider how an extended analysis ought to be performed on the KATRIN output in order to get reliable results.

We present here one approach which seems to give several advantages over the standard frequentist analysis that has been used so far. In Sec. II we describe our analysis methods before presenting results for a number of cases in Sec. III. Finally, we give some concluding remarks in the last section.

II. METHODS: FREQUENTIST AND BAYESIAN ANALYSIS TOOLS**A. The principles of Mainz and KATRIN data analysis**

Let us begin by summarizing the procedures for production and analysis of KATRIN spectra as performed by a toy model Monte Carlo and analysis code for KATRIN-like experiments [2]. This code has previously been used to forecast the experiment’s sensitivity to the neutrino mass [7].

Because KATRIN has an integrating spectrometer [a consequence of the (magnetic adiabatic collimation with electrostatic (MAC-E) filter technique], the β spectrum must be written as an integral over the electron energy [see Eq. (2)]. Here U is the retarding potential of the spectrometer, N_{tot} is the total number of tritium nuclei in the source, t_U is the measurement time allotted for a given value of the retarding potential, and f_{res} is the experimental response function (which in turn is a combination of the electron energy loss function of the tritium source and the transmission function of the

spectrometer). $\frac{dN_\beta}{dE_e}$ is the theoretical β spectrum folded with the electronic final state distribution of molecular tritium.

A retarding voltage-independent background rate of B_0 is now added to Eq. (2),

$$N_s(qU, E_0, m_{\nu_e}^2) = N_{\text{tot}} t_U \int_0^{E_0} \frac{dN_\beta}{dE_e}(E_0, m_{\nu_e}^2) \times f_{\text{res}}(E_e, qU) dE_e. \quad (2)$$

$$N_{\text{exp}}(qU) = N_s(qU, E_{0,0}, m_{\nu_e,0}^2) + N_b + \text{Rnd}[Gauss(\sigma, \mu)]. \quad (3)$$

$$N_{\text{fit}}(qU, A, B, E_0, m_{\nu_e}^2) = A \frac{N_s(qU, E_0, m_{\nu_e}^2)}{A_0} + B \frac{N_b}{B_0}. \quad (4)$$

$$\chi^2(A, B, E_0, m_{\nu_e}^2) = \sum_i \left(\frac{N_{\text{exp}}(qU_i) - N_{\text{fit}}(qU_i, A, B, E_0, m_{\nu_e}^2)}{\sigma(qU_i)} \right)^2, \quad (5)$$

giving us the following theoretical expression for a KATRIN-like spectrum:

$$N_{\text{th}}(qU, E_0, m_{\nu_e}^2) = N_s(qU, E_0, m_{\nu_e}^2) + N_b, \quad (6)$$

where N_b is the product of B_0 and the measurement time t_U .

Individual spectra (to resemble the real measurements) are built using initial parameters $m_{\nu_e,0}^2$ and $E_{0,0}$ for the neutrino mass-squared and the endpoint energy. To the theoretical expression is then added a random component from a Gaussian distribution with $\sigma(qU) = \sqrt{N_s + N_b}$ and $\mu(qU) = N_s + N_b$. These ‘‘experimental’’ spectra are described by Eq. (3).

When we want to fit our randomized β spectra we have to account for statistical fluctuations by allowing the overall amplitude A of the signal as well as the background rate B to vary against the theoretical amplitude A_0 and background rate B_0 . In addition, we allow the neutrino mass-squared $m_{\nu_e}^2$ as well as the endpoint energy E_0 to deviate from the initial parameters of the simulation $m_{\nu_e,0}^2$ and $E_{0,0}$. This is expressed in Eq. (4). By combining Eqs. (3) and (4) we finally get KATRIN’s χ^2 function [2] [see Eq. (5)].

The analysis of the simulated data can be performed with MINUIT2, which is imbedded in the ROOT package. This procedure performs a minimization of the χ^2 function using the combined minimizer package. The combined minimizer in turn uses either an evaluation of the covariance matrix or a simplex method to find the best minimum of the χ^2 function in the parameter space [8]. One can now do a standard frequentist analysis to find the statistical uncertainty on, e.g., the neutrino mass by producing a suitable amount of Monte Carlo spectra, performing the minimization for each of them, and finally, inspecting the resulting histograms. An example is shown in Fig. 1 for 12 860 spectra produced with $m_{\nu_e} = 0.0$ eV.

This minimization approach works just fine for the four well-known free parameters used in a standard KATRIN analysis (see Table I). However, as previously indicated the minimization approach has a number of drawbacks. For one thing it does not give any information on multiple minima, and it is not well suited for finding shallow minima. Furthermore, extracting detailed information on correlated parameters is pretty laborious.

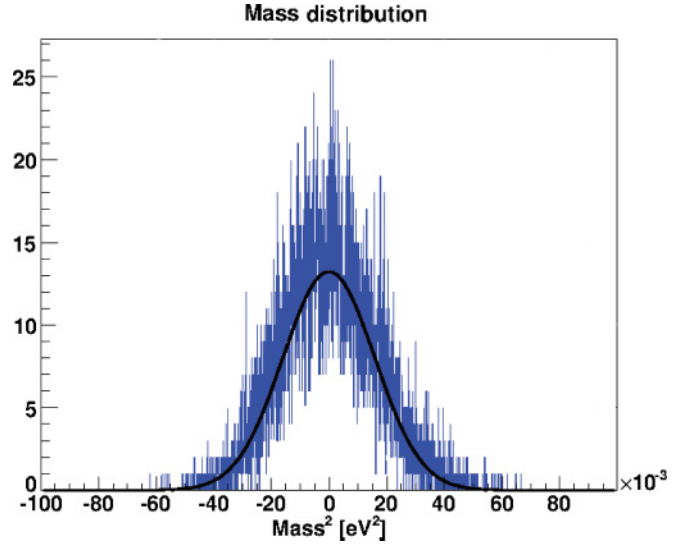


FIG. 1. (Color online) An example histogram depicting the neutrino mass-squared values from minimizations of 12 860 β spectra for a KATRIN-like parameter set and an assumed value for the neutrino mass of $m_{\nu_e} = 0$ measured with an optimized time distribution over the last 25 eV of the β spectrum, e.g., compare to [7]. The histogram has been fitted with a Gauss function, and the results of this analysis were $m_{\nu_e}^2 = -9.184 \times 10^{-5}$ and $\sigma(m_{\nu_e}^2) = 0.01591$ with $\chi^2/ndf = 1.0033$.

These problems can of course be addressed in a frequentist context. For one thing, MINUIT2 offers several different minimization tools and programs could easily be written to produce two-dimensional (2D) likelihoods, etc., that could be inspected in order to see parameter correlations and multiple minima. However, as we add more parameters the minimization procedure often becomes problematic and rather slow. We have therefore investigated the Bayesian approach described in the next section for the following reasons:

- (i) We need not assume any shape of the parameter distributions, and can, for instance, easily handle non-Gaussian parameters.
- (ii) COSMOMC is designed to do parameter estimation in cosmology using many large datasets. The code therefore routinely handles 12 or more parameter dimensions, and we do not have to worry that the analysis becomes unmanageably slow if we wish to include nonstandard physics in the analysis.
- (iii) By using COSMOMC [9], which is a free and publicly available code, we can take advantage of the

TABLE I. KATRIN standard analysis parameters. Please note, that we show and plot the deviation of the value of the endpoint of the β spectrum from the theoretically expected value: $E_0 = 18575$ eV.

Parameter	Unit	Typical input value
$m_{\nu_e,0}^2$	eV ²	0.0 – 1.0
$\Delta E_{0,0}$	eV	0.0
B_0	Hz	0.01
A_0	Hz	477.5

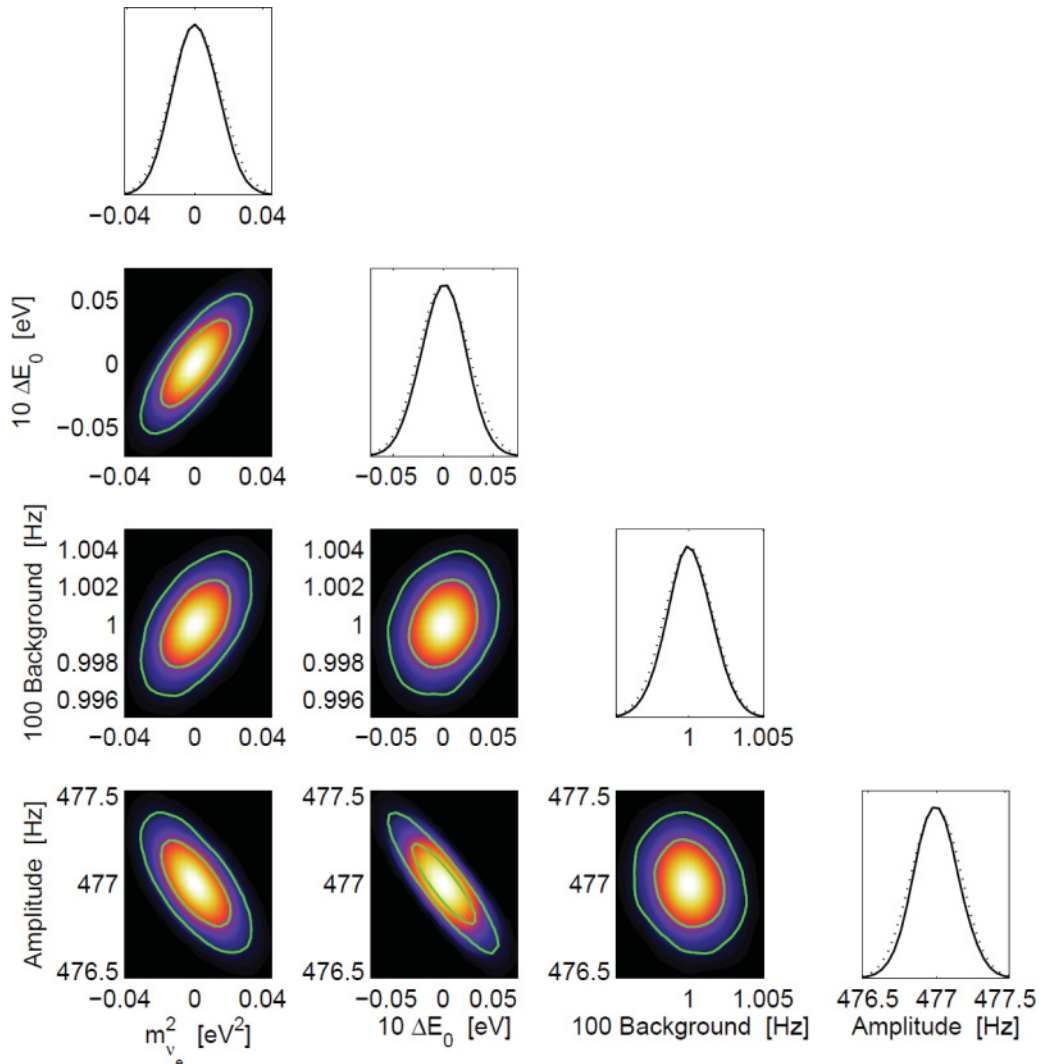


FIG. 2. (Color online) A one-neutrino analysis with input mass $m_{\nu_e,0} = 0.0$ eV. In the COSMOMC output the contours (dotted lines) mark the likelihood function in the 2D (1D) posterior distributions. The shading (full lines) marks the number of times the MCMC procedure has probed a specific area of the parameter space. The results have converged nicely and gives $m_\nu^2 = -0.41 \times 10^{-5} \pm 0.013$ eV².

automatically produced MATLAB files to inspect a graphic representation of the 2D likelihood contours. We even get the best-fit values and standard deviations as output. Put differently, we do not need to write much additional code in order to get the analysis advantages we were looking for.

To be clear, there are no fundamental problems in doing a frequentist analysis on KATRIN datasets, especially since the number of free parameters is reasonably small in the standard analysis. However, we believe the task can be done in a faster and more elegant fashion using COSMOMC.

B. Bayesian parameter inference with COSMOMC

The key ingredient in COSMOMC is the Markov chain Monte Carlo (MCMC) and Bayesian inference techniques. As mentioned, the program is built with the intention of inferring

cosmological parameter values and comparing cosmological models using large cosmological datasets (such as Cosmic Microwave Background (CMB) data from Wilkinson Microwave Anisotropy Probe (WMAP) and supernova surveys). But in principle COSMOMC can analyze whatever data set the user provides—the cosmology can simply be “turned off” if it is irrelevant. Note also that our purpose here is not model comparison but purely parameter inference. We can then compare the best-fit value and statistical error from our method with the results of a typical frequentist analysis without further concerns that quantities such as goodness of fit (i.e., the absolute best fit χ^2) does not have a simple interpretation in Bayesian analysis.

COSMOMC uses a Bayesian statistics approach to the analysis. When doing so called Bayesian parameter inference one is interested in knowing the posterior probability, $P(\bar{\theta}|D, M)$ —the probability of the parameters $\bar{\theta}$ given the data D and the model M . The inverse question is for the probability of the data, D , given the parameters and the model, $P(D|\bar{\theta}, M)$ —this is

simply the likelihood function. With these two probabilities and the well-known Bayes theorem,

$$P(A \wedge B) = P(A) \cdot P(B|A) = P(B) \cdot P(A|B), \quad (7)$$

one can write an expression for the posterior probability:

$$P(\bar{\theta}|D, M) = \frac{L(D|\bar{\theta}, M) \cdot \pi(\bar{\theta}|M)}{\varepsilon(D|M)}. \quad (8)$$

Here L is the likelihood, which can be easily derived from the χ^2 function.¹ The posterior probability is thus proportional to the likelihood.

Meanwhile $\pi(\bar{\theta}|M)$ is the so-called prior probability, sometimes referred to as the subjective input; it is what we believe we know from theory before even taking the data into account. Correspondingly, this probability has no dependence on the data. Note that we have been using flat priors on all input parameters in this paper. This is a quite typical way of stating that we do *not* have any prior knowledge of the parameters in question; however, in the case of the neutrino mass the choice was intentional and built on the investigations by Høst *et al.* [10]. This paper showed the best agreement between frequentist and Bayesian methods, on the best-fit value for $m_{\nu_e}^2$ for $m_{\nu_e} \sim 0$ eV, when a flat prior on the mass squared was used. Note also that our prior on $m_{\nu_e}^2$ is uniform across $m_{\nu_e} = 0$ eV and into the negative parameter space. This is in agreement with previous analysis conventions of the Troitsk, Mainz, and KATRIN Collaborations. So in principle one could use a prior with a physical cutoff at $m_{\nu_e} = 0$ eV, but since the purpose of this paper is to compare the methods used, we have kept the flat symmetric prior in all our calculations.

Finally, $\varepsilon(D|M)$, the evidence, is in effect only a parameter-independent normalization constant² [11].

When we want to know the best-fit values and confidence levels of specific parameters, we can simply integrate over all the remaining (nuisance) parameters. This is called marginalization, and the output is called the marginalized probability for the parameter of interest.

In addition to this rather convenient production of parameter probability distributions, from the Bayesian inference approach, COSMOMC gives us another great advantage by using the MCMC to probe the parameter space. This will provide a very thorough and easy-to-inspect mapping of the parameter space of interest.

The purpose of the MCMC is to probe the whole parameter space in a randomized manner. To achieve this one implements the Metropolis Hastings algorithm [12] consisting of three main steps:

- (i) First, an initial point $\bar{\theta}_0$ is chosen.
- (ii) Second, a step is proposed in some random direction, after which the new point is evaluated: $P(\bar{\theta}_i + \bar{\theta}_p)$.

Here $\bar{\theta}_i$ means the iterative point, while $\bar{\theta}_p$ is the proposed addition taken from some proposal density.

- (iii) Finally, the procedure decides whether or not to take the step. The point $\bar{\theta}_i + \bar{\theta}_p$ is accepted if the posterior probability is improved, that is, if

$$\frac{P(\bar{\theta}_i + \bar{\theta}_p)}{P(\bar{\theta}_i)} \geq 1. \quad (9)$$

If the expression above is <1 , the step is accepted with some probability r (rejected with probability $1 - r$). In this manner we generate a set of points $\{\bar{\theta}_i\}$, also called a Markov chain. For the number of points N going to infinity, we thus have a representation of the posterior probability.

The decision procedure of the Metropolis Hastings algorithm allows the chain to wander away from any local minimum and thus potentially discover other minima (to a degree determined by the value of r ³). On the other hand, it also guarantees that the parameter space near the minimum is very well probed. Furthermore, one can perform the analysis on a combination of multiple chains—all started at random positions—and get an even better picture of the behavior of the different parameters in the allowed intervals. To get rid of unphysical effects from the random starting points, one normally allows for a burn-in, i.e., the first part of the Markov Chain is removed. In our case the burn-in is 50% of the sample size.

Before running the program one must carefully choose step sizes and parameter ranges. Several settings in both the COSMOMC program as such and in the parameter files can be tweaked to fit one's purpose.

Unfortunately, it is in principle impossible to determine in any absolute terms whether or not a specific chain has converged [12], but various convergence diagnostics have been developed. For instance, when analyzing multiple chains a convergence parameter R , defined as the variance of the chain means divided by the mean of the chain variances, can be evaluated. If $1 - R$ is less than some chosen small number (in our case 0.03), this information is interpreted as good convergence. When COSMOMC has generated the chains we need, the data analysis is performed, giving us best-fit values and standard deviations for all the parameters.

Additionally, COSMOMC produces a number of useful MATLAB files which can be used to produce one-dimensional (1D) and 2D plots of the marginalized distributions. Inspecting this graphical output allows us to determine if the chains have really converged, whether there are multiple minima, and perhaps most importantly, it shows parameter correlations right away.⁴

If we go through all of this for say a single Monte Carlo generated β spectrum we get all the nice advantages mentioned

¹The likelihood function L is connected to the χ^2 function in the following way: $L = \exp(-\chi^2/2)$. This implies that a Gaussian sampling distribution is being used for the selection MCMC data points, but crucially, the likelihood and posterior functions are not themselves Gaussian.

²However, it can be important in some contexts, e.g., in comparing two qualitatively different models.

³In our case r is defined as $e^{\Delta\chi^2/2T}$, with temperature $T = 1$.

⁴In fact, COSMOMC—or rather GETDIST—produces a multitude of diagnostics files in addition to the graphical output. More information on these can be found on the COSMOMC homepage [9]. Besides, it is fairly easy to edit the GETDIST program to produce output files that fit one's purpose.

TABLE II. The statistical uncertainty on the neutrino mass squared for 11 different input values. The second row has been calculated using the Bayesian approach in the COSMOMC analysis, while the third row has been calculated in the usual frequentist approach assuming a Gaussian distribution function.

m_{ν_e} [eV]	0.0	0.1	0.2	0.3	0.4	0.5	0.6	0.7	0.8	0.9	1.0
$\sigma_{\text{stat,bay}} [10^{-2} \text{ eV}^2]$	1.31	1.34	1.38	1.39	1.45	1.51	1.53	1.59	1.61	1.66	1.69
$\sigma_{\text{stat,fre}} [10^{-2} \text{ eV}^2]$	1.64	1.70	1.79	1.95	1.88	1.91	1.93	2.04	2.02	2.09	2.21

above. But the analysis of that one spectrum would take many hours as compared to minutes or seconds with the MINUIT2 procedure, and we would mostly just have achieved a much slower evaluation of the best-fit values for that particular spectrum. However, if we instead use the theoretical β spectrum⁵ as our input data but with Monte Carlo-generated error bars, our best-fit values and standard deviations from COSMOMC should correspond to the results of the frequentist approach of building histograms for a very large (going to infinity) number of measurements.

To recap, we implemented our χ^2 function for KATRIN-like experiments in COSMOMC and simply turned off cosmology. We have used the theoretical spectrum for any given model as a data set, with the Monte Carlo-generated error bars of the original code. The results are discussed in the following section.

III. RESULTS

A. The minimal model

As a first test of our methods we have attempted to reproduce the KATRIN sensitivity. We thus generated a tritium β spectrum using as input so far only four parameters: the electron neutrino mass-squared $m_{\nu_e,0}^2$, the endpoint of the β spectrum $E_{0,0}$,⁶ the background count rate B_0 , and the signal count rate near the β -spectrum endpoint A_0 [see Eq. (6)].

The input signal count rate can be calculated as a combination of the column density of the source and the magnetic fields and cross sections of the spectrometer and source. In our case the count rate near the endpoint E_0 is included in the analysis code via an amplitude factor A_0 as in Eq. (4). The exact definition and full calculation of this factor A_0 is included in Appendix A of Ref. [14]. Given KATRIN's experimental settings, the amplitude has the value $A_0 = 477.5$ Hz.

We would like to remark that the value of the endpoint energy E_0 needs to be treated as a free parameter to produce

realistic fits with respect to fitting of $m_{\nu_e}^2$. Until now the $^3\text{He} - ^3\text{H}$ mass difference is known from precision Penning trap experiments with 1.2-eV precision [15], but already the fits of the experiments at Mainz [3] and Troitsk [4] would have needed a much more precise input value to justify keeping E_0 fixed in the fit.

The values of our free parameters are listed in Table I.

The COSMOMC results for a theoretical spectrum with $m_{\nu_e,0} = 0.0$ eV are presented in Fig. 2. Clearly the chains have converged nicely in this case and the parameters seem well-constrained. The output values of our analysis are

$$m_{\nu_e}^2 = (-0.41 \cdot 10^{-5} \pm 0.013) \text{ eV}^2$$

$$\Delta E_0 = (0.87 \cdot 10^{-5} \pm 0.22 \cdot 10^{-2}) \text{ eV}$$

$$B = (1.00 \cdot 10^{-2} \pm 0.15 \cdot 10^{-4}) \text{ Hz}$$

$$A = (477.0 \pm 0.16) \text{ Hz.}$$

Here, the error bars represent a 1σ deviation from the best-fit value and thus represent the interval containing the central 68% of the integral of the distribution function.

We note that our analysis gives a statistical error on the neutrino mass squared of 0.013 eV^2 , but the statistical uncertainty from the frequentist analysis shown in Fig. 1 is 0.016 eV^2 and thus $\approx 23\%$ larger than our Bayesian result.⁷

However, the procedure with which we find the standard deviations of the parameters (through a marginalization over nuisance parameters) is very different from a frequentist approach and in general, one would not expect the two methods to return the same uncertainties. A small comparison of the statistical error bar for 11 different values of the neutrino mass in a frequentist and a Bayesian analysis (see Table II) shows us that in this case one gets a systematically higher value of the statistical uncertainty when using frequentist methods for the calculation. We checked that this is not caused by any problems in the code, seeing as the two approaches agree on

⁵The theoretical input values should represent the average of infinitely many measurements or Monte Carlo realizations (see also [13]).

⁶To suppress the number of digits, we rather plot and write its deviation from 18575 eV , i.e., ΔE_0 .

⁷One can calculate KATRIN's sensitivity to the electron neutrino mass at 90% C.L. using the following equation (and assuming a Gaussian distribution function): $L = \sqrt{1.64} \sqrt{\sigma_{\text{tot}}^2(m_{\nu_e}^2)}$. Here $\sigma_{\text{tot}}^2(m_{\nu_e}^2) = \sigma_{\text{stat}}^2 + \sigma_{\text{sys}}^2$, and KATRIN's systematic error on the neutrino mass squared is the 0.017 eV^2 quoted in [2]. The Bayesian analysis gives $\sigma_{\text{stat}}^2 = 0.013 \text{ eV}^2$ and a sensitivity of 0.19 eV (90% C.L.) on the electron neutrino mass.

TABLE III. Amplitudes investigated in the sensitivity plot presented in Fig. 4.

Amplitude [Hz]	2.0	4.0	8.0	16.0	32.0	64.0	125.0	250.0	500.0	1000.0
----------------	-----	-----	-----	------	------	------	-------	-------	-------	--------

TABLE IV. Energy resolutions investigated in the sensitivity plot presented in Fig. 4.

Energy resolution [eV]	0.5	1.0	2.0	4.0

the χ^2 value. By inspecting the likelihood contours of Fig. 2 we can also see that the smaller Bayesian statistical uncertainty is *not* caused by any cutoff effects on the prior (the likelihoods have all converged within the relevant parameter interval). So even with almost normal distributions we must conclude that we do not get the same uncertainties and that this is quite simply due to using two different statistical approaches. (For a thorough treatment of this issue, see also [16].)

We do, however, get the correct output values and the right trend in the behavior of $\sigma_{\text{stat}}(m_{\nu_e}^2)$ as demonstrated in Table II. In conclusion, the COSMOMC approach seems to produce robust results.

B. Sensitivity plot

As a first application of our Bayesian analysis formalism we have built a sensitivity plot for KATRIN-like experiments, or rather, an illustration of the behavior of the statistical uncertainty on the neutrino mass squared as a function of key experimental settings. The sensitivity to the electron neutrino mass of a KATRIN-like experiment depends on the signal strength, the background count rate, and the energy resolution of the experiment. Given the fairly well understood effect of the background on the sensitivity, we investigate only the effect of the signal strength and the energy resolution. The specific values used are listed in Tables III and IV. Additionally, we include an optimization of the measurement time distribution for each of our KATRIN-like experiments (as specified by their amplitude and energy resolution). This optimization has in fact a great deal of influence on the reachable sensitivity of such an experiment. Currently KATRIN is projected to have a runtime of three years, but because of experimental stability issues the measurements are performed as a relatively fast scan over the electron energies of interest (or rather retarding voltages) of total duration 966 s. The measurement time allotted to each data point, the t_U in Eq. (2), has been carefully optimized for KATRIN's experimental settings as described in [2].

The basic structure of the measurement time distribution can be represented as three segments around the region of the β -spectrum endpoint.

- (i) First, one needs measurements up to about 10 eV above the endpoint of the β spectrum to determine the correct background.
- (ii) Second, the “bulk” region of interest below the endpoint of the β spectrum must be treated carefully. Effectively this is the section we optimize.
- (iii) Third, previous investigations by the KATRIN Collaboration have pointed out that there exists a region of

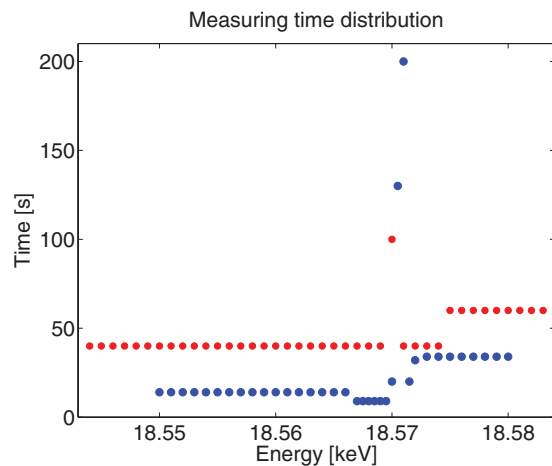


FIG. 3. (Color online) The blue circles represent the standard KATRIN measurement time distribution and the red circles show an example of a simplified time distribution with measurement points separated by 1 eV in the main block. This particular time distribution contains only one point in the range: $0.02 \text{ Hz} < N_{th}(qU, E_0, m_{\nu_e}^2) < 0.04 \text{ Hz}$.

maximal sensitivity to the neutrino mass. This region is centered around the electron energy for which the signal count rate equals 2 times the background count rate: $N_s = 2N_b$ [17]. Above this narrow region the total count rate is dominated by background noise. Below it the sensitivity to the neutrino mass drops as one goes away from the endpoint. Therefore extra measurement time is devoted to measurements in this interval. Given the projected KATRIN background count rate of 0.01 Hz, the total count rate of the critical point must be 0.03 Hz.

As a rule we construct the background block of our distribution as ten points separated by 1 eV, each having $t_U = 60$ s. The main block contains a total of 30 points with varied spacing (to be optimized) and $t_U = 40$ s. Finally 60 s are added to t_U for $0.02 \text{ Hz} \leq N_{th}(qU, E_0, m_{\nu_e}^2) \leq 0.04 \text{ Hz}$. We find that the 40-100-60 block structure does a good job of simulating both the structure and total duration of the measurement time distribution while still being simple enough to manipulate. For the sake of comparison we show the fully optimized KATRIN measurement time distribution and one of our simplified distributions in Fig. 3.

To build the sensitivity plot we let a script evaluate $\sigma_{\text{stat}}(m_{\nu_e}^2)$ for all energy resolutions given a specific amplitude. The evaluation includes an optimization of the measurement time distribution: For the first energy resolution we find the best statistical uncertainty using all the available distributions [as specified by their data point intervals in the main block (see Table V)]. We then impose a time-saving condition stating that the next energy resolution is allowed only to use the previous best distribution and its closest neighbors, and so on

TABLE V. The allowed data-point intervals used in the main block of our measurement time distributions.

Data-point intervals [eV]	0.1	0.2	0.4	0.8	1.0	1.2	1.4	1.6	1.8	2.0

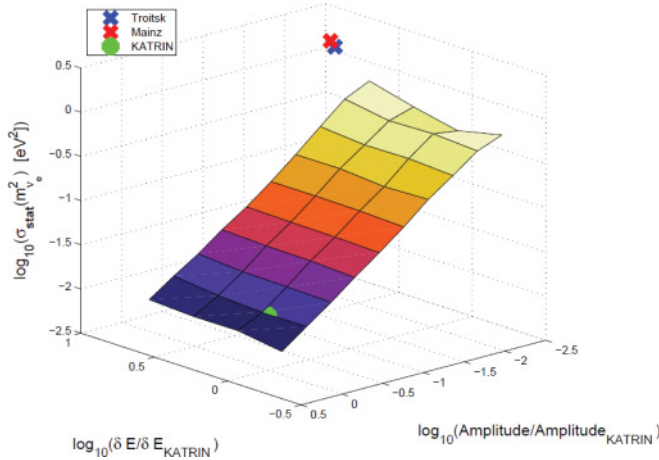


FIG. 4. (Color online) Our final sensitivity plot result showing the statistical uncertainty on the neutrino mass squared as a function of amplitude and energy resolution for a KATRIN-like experiment. It is very clear from the figure that $\sigma_{\text{stat}}(m_{\nu_e}^2)$ is strongly dependent on the signal count rate (as could be expected) and to a much lesser degree on the energy resolution, δE . For comparison the figure also show the corresponding statistical uncertainties of the Troitsk, Mainz, and KATRIN experiments. (The KATRIN point was calculated with the COSMOMC approach presented here.)

for the remaining energy resolutions. The reason for doing this “spline” between energy resolutions and not between amplitudes is the expectation that the largest sensitivity fluctuations will take place in the amplitude direction.

We present the average of ten sensitivity plots as our result in Fig. 4, including points corresponding to the statistical uncertainty of the Mainz [3] and Troitsk [4] experiments. The figure shows a clear log-log dependence of $\sigma_{\text{stat}}(m_{\nu_e}^2)$ on the amplitude. The dependence on the energy resolution on the other hand is very weak. Making a fit to the plane of the sensitivity plot gives us

$$\log_{10} [\sigma_{\text{stat}}(m_{\nu_e}^2)] = 0.058 \log_{10}(\delta E) - 0.70 \log_{10}(\text{Amp}) + 0.0038. \quad (10)$$

That is roughly a factor of 12 stronger dependency on the amplitude than on the energy resolution in this fit (with $R_{\text{fit}}^2 = 0.9989$). Note that these simulations are done without considering the corresponding systematics, which would most likely give a stronger dependence on the energy resolution ΔE .

Furthermore, the statistical uncertainties from the Troitsk and Mainz experiments (2.5 and 2.2 eV^2 , respectively, taken from their final results) are somewhat above the plane. This is as could be expected, given the fact that the plot was built specifically from a KATRIN toy model. And as mentioned above we get systematically lower statistical uncertainties using our Bayesian analysis algorithm than from corresponding frequentist methods.

Finally, we noted a tendency in our procedure to choose large data-point separations for the optimal measurement time distribution. This effect, a lower statistical uncertainty caused by analyzing a larger energy interval below the Q value, was already demonstrated in Fig. 19 of [1]. For our purpose we have

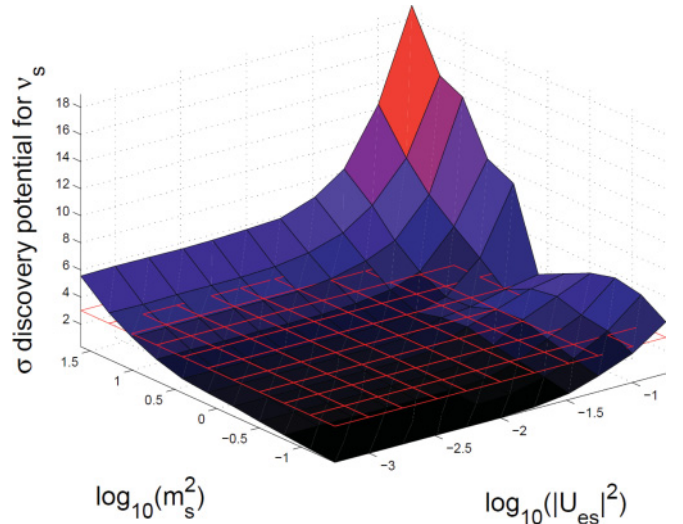


FIG. 5. (Color online) This figure shows the σ detection potential of the massive sterile neutrino for the standard KATRIN-like settings. The x and y axis depicts the logarithm of the sterile mass squared and the mixing weight and the red mesh illustrates the 3σ level. As one would expect, the mass and the mixing weight must be rather high in order to get a good detection of the sterile component.

kept the systematic uncertainty at 0.017 eV^2 , as projected for the KATRIN experiment [2], and our sensitivity (so to speak) depends only on the statistical uncertainty.

C. Sterile neutrinos

After these initial tests of our COSMOMC extension we have tried adding further parameters in our routine.

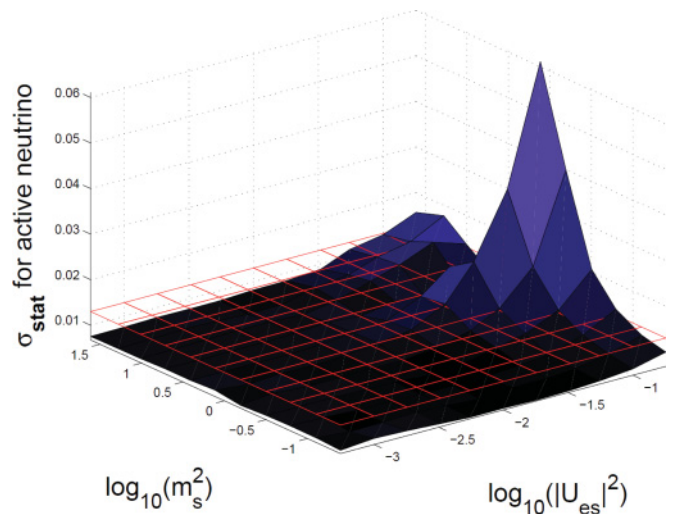


FIG. 6. (Color online) Shown here is the statistical uncertainty (in eV^2) on the massless neutrino component. Again the x and y axis depicts the logarithm of the sterile mass squared and the mixing weight, but this time the red mesh depicts the standard one-neutrino statistical uncertainty of around 0.013 eV^2 (for this analysis method). The features visible in this and the previous figure are explained in much greater detail in Ref. [14].

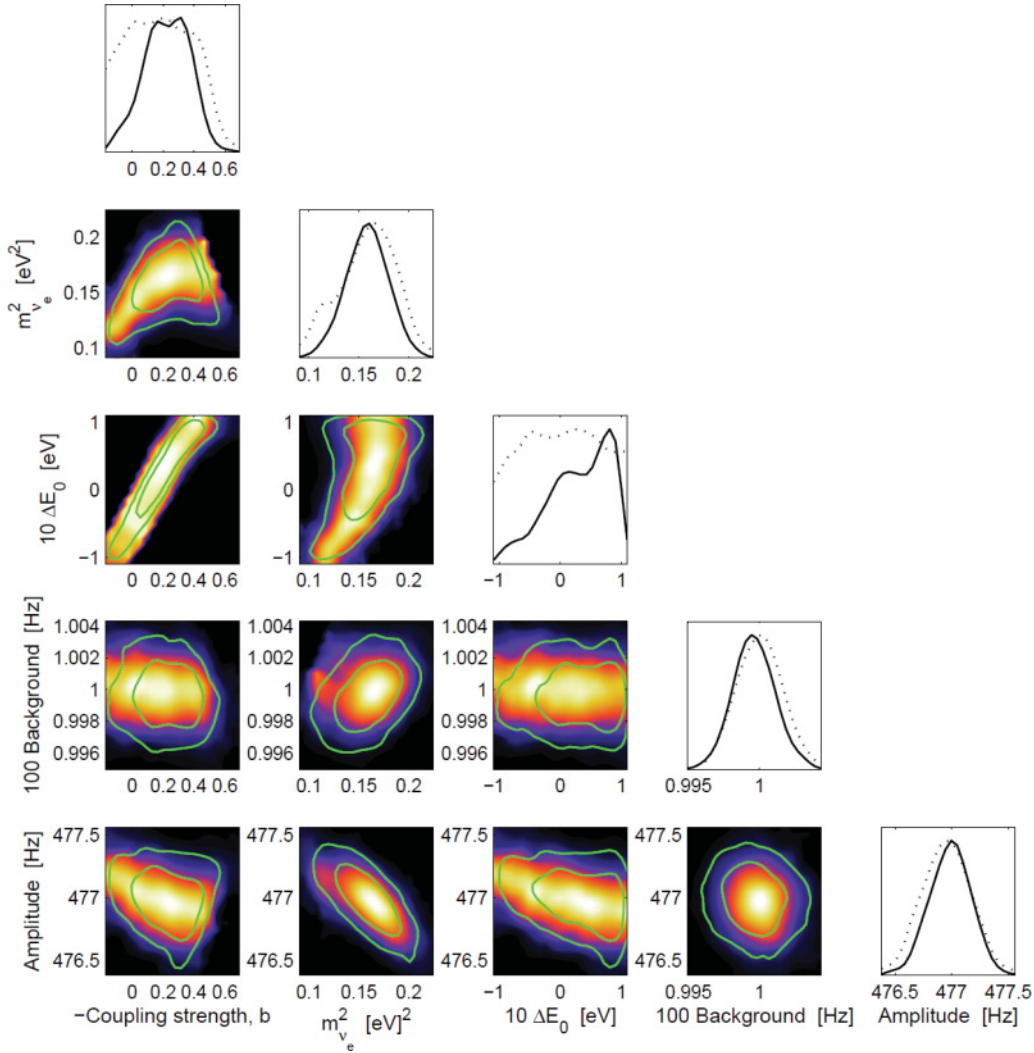


FIG. 7. (Color online) A typical COSMOMC output for a model with $b_0 = -0.13$ and $m_{\nu_e,0} = 0.4$ eV. One clearly sees the correlations between m_{ν_e} , b , and ΔE_0 . Despite quite large input parameter ranges for $m_{\nu_e}^2$ and b , neither is well constrained.

As previously mentioned it is obvious that KATRIN cannot resolve the mass-squared differences between the known active states of $\Delta m_{12}^2 = 8 \times 10^{-5}$ eV² and $\Delta m_{23}^2 = |2.6 \times 10^{-3}|$ eV², respectively. However, sterile neutrinos with mass states in the electronvolt range could in principle mix with $\bar{\nu}_e$. Such neutrinos would provide a much better target for direct detection in β -decay experiments than the active neutrinos which are expected to have subelectronvolt masses. Their relatively high mass would allow for an easy separation from the primary decay signal in experiments such as KATRIN.

Recently the MiniBooNE Collaboration confirmed their findings from 2007 [18] and more indications of a fourth mass state can be found in the so-called reactor anomaly [19,20]. Even cosmology suggests an effective number of neutrino species slightly larger than three [16,21–23]. We have therefore performed a more thorough investigation of the possible detection potential for sterile neutrinos by KATRIN-like experiments. For the total results see [14] and references therein.

Here we present only our main results for effectively a 1+1 (active + sterile) neutrino scenario. We can justify having only one active neutrino by the known mass-squared differences. We kept the active neutrino massless and performed the analysis for a broad range of sterile neutrino masses. For KATRIN's standard settings (see Table I) we get the results presented in Figs. 5 and 6.

We found that KATRIN should be able to perform a 3σ detection of any of the heavy mass states we used as long as $|U_{es}|^2 \gtrsim 0.055$. Likewise, a 1σ detection is achievable for $|U_{es}|^2 \gtrsim 0.018$.

D. Right-handed currents

As a final application we take a look at right-handed currents. We use the notation of Stephenson *et al.* in [24] and let b parametrize the strength of the right-handed interaction. We define $b = \rho_R \cos \theta_R / \cos \theta$, where $\cos \theta$ is the mixing

TABLE VI. Input neutrino masses and right-handed coupling strengths used to produce figures.

m_{ν_e} [eV]	0.0	0.1	0.2	0.3	0.4	0.5	0.6	0.7	0.8	0.9	1.0
b	-0.19	-0.16	-0.13	-0.10	-0.07	0.0	0.07	0.10	0.13	0.16	0.19

angle from the mass eigenstate to the left-handed current weak eigenstate and $\cos\theta_R$ is the mixing angle from the mass eigenstate to the corresponding right-handed current weak eigenstate. Again we assume for simplicity that the mass of the electron neutrino can be described by one effective mass eigenstate. ρ_R is the ratio of the effective strength of interactions mediated by right-handed currents to the strength of interactions mediated by the well-known left-handed weak current. Then the differential β spectrum is modified in the following way in the presence of right-handed currents [24]⁸:

$$\frac{dN_\beta}{dE_e} = E_\nu \sqrt{(E_\nu^2 - m_\nu^2)} \left(1 + 2 \frac{b}{1+b^2} \frac{m_\nu}{E_\nu} \right). \quad (11)$$

From many data of weak precision experiments reviewed in Ref. [25], Bonn *et al.* derive an upper limit on $|\frac{2b}{1+b^2}|$ of 0.31 (99.7% C.L.) [26], translating to $|b| \lesssim 0.16$ in our parametrization.⁹ It is clear from Eq. (11) that the mass and the coupling parameter b are strongly correlated. Combined with the well-known correlation between the neutrino mass

⁸Note that the last term is equivalent to 2 times the similar expression in [26] in the limit of small b . We wish, however, to use Eq. (11) retaining the physical meaning of b , rather than treating the coupling as an effective parameter.

⁹However, it is clear that if $|\frac{2b}{1+b^2}| < 0.31$ can also give the limit $|b| \gtrsim 6.3$, obviously the effect of $b \sim 0$ and $|b| \gg 1$ would give very similar spectra using Eq. (11). However $b > 1$ has no physical meaning, cf. our definition.

squared $m_{\nu_e}^2$ and the endpoint energy ΔE_0 [5], this will propagate to an additional b - ΔE_0 correlation. Figure 7 shows a COSMOMC output for all the parameters in a model with input values $b_0 = -0.13$ and $m_{\nu_e,0} = 0.4$. The input parameter ranges were $m_{\nu_e,0}^2 \pm 1.5 \text{ eV}^2$ and $-2.5 < b_0 < 2.5$, respectively. We see that even within these rather large conservative intervals, neither m_{ν_e} or b can be determined well.

As another example Fig. 8 shows the behavior of the m_{ν_e} - b correlation for a range of masses and $b_0 = \pm 0.13$. Oddly enough, for small input masses this allows for a better $\sigma_{\text{stat}}(m_{\nu_e}^2)$ than in the purely left-handed case, if the right-handed coupling constant b is known. We believe this is caused by the large available phase-space in the b direction. This means the likelihood can be made very narrow around the input value while still providing many valid solutions; in other words, it is a numerical effect. However, we also notice that when KATRIN's sensitivity is reached the uncertainty on the mass will be determined again by the experimental limitations and not by numerical solutions. Therefore the correlation between $m_{\nu_e}^2$ and b reappears.

Given these disconcerting initial results we investigated how large an influence the presence of right-handed currents might have on the output neutrino mass. We have performed the full COSMOMC analysis for the parameters given in Table VI. For $b = 0$ the analysis was the standard analysis, i.e., without a b dimension. Our main results are presented as a relative bias compared to the $b = 0$ case (with the exclusion of $m_{\nu_e} = 0$ in

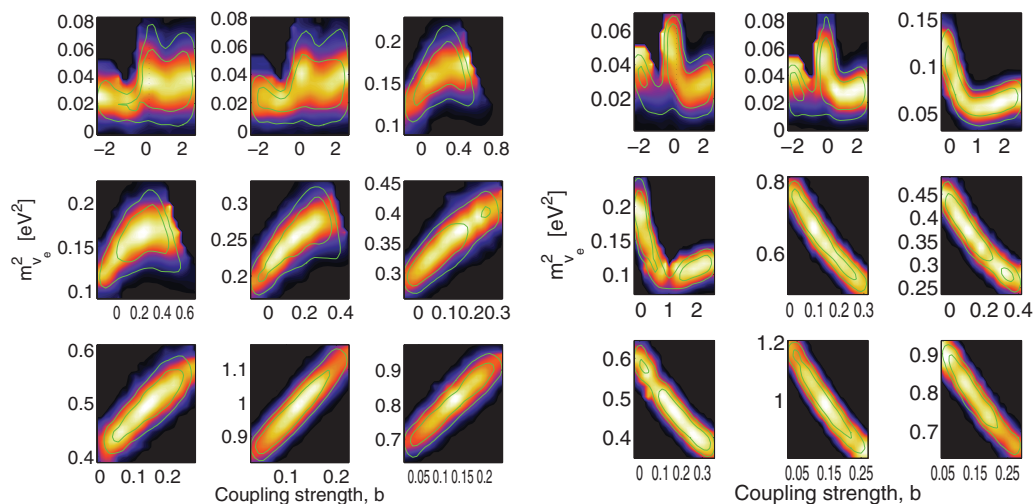


FIG. 8. (Color online) The left figure shows marginalized COSMOMC 2D likelihood contours and MCMC data for models with $b_0 = -0.13$ and $m_{\nu_e,0}$ ranging from 0.1 eV to 0.9 eV (going from the upper left corner to the lower right corner). The right figure has $b_0 = 0.13$ and the same range of input masses. The correlation between m_{ν_e} and b only establishes itself when the neutrino mass is larger than KATRIN's sensitivity of 0.2 eV. This allows for smaller $\sigma_{\text{stat}}(m_{\nu_e}^2)$ than in the case of $b_0 = 0$, because the MCMC routine lets the uncertainty on the mass fill the extra parameter dimension (b).

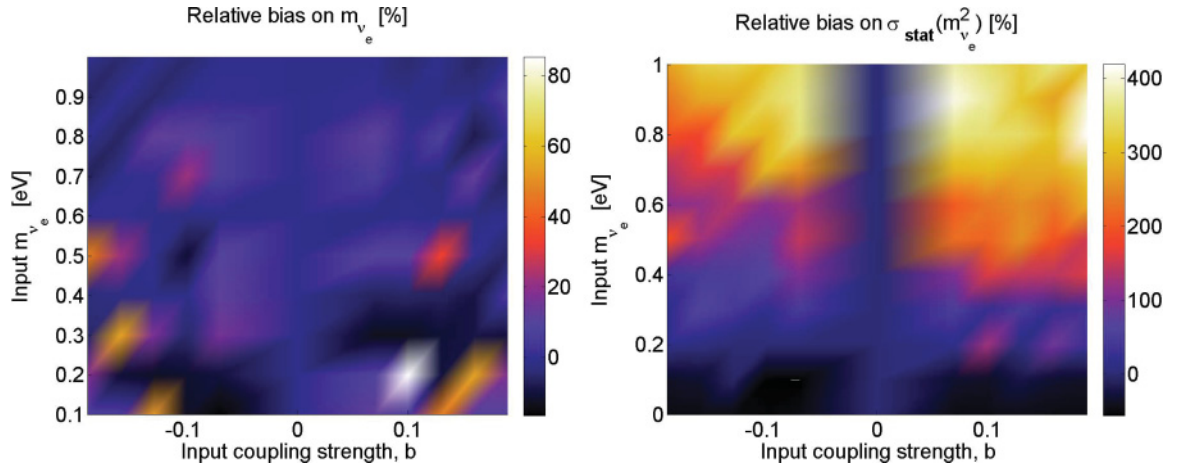


FIG. 9. (Color online) The left figure shows the bias on m_{ν_e} as compared to the case without right-handed couplings and the right figure shows the bias on $\sigma_{\text{stat}}(m_{\nu_e}^2)$. This analysis includes the right-handed coupling strength as a free parameter. The bias on the mass is as large as 80%, while the values of $\sigma_{\text{stat}}(m_{\nu_e}^2)$ is up to five times as large as for the standard case (barring the parameter range below KATRIN's sensitivity where the uncertainty on the mass parameter migrates into the b dimension in the MCMC).

the mass bias, to avoid infinities). The results are shown in Figs. 9 and 10. Note that we included $b = |0.19|$ to create a better overview of the behavior of $m_{\nu_e}^2$.

The results shows us first that the output mass values fluctuate rather wildly and in some cases deviate by as much as $\approx 80\%$ from the input values as shown in the left panel of Fig. 9. And secondly, the statistical uncertainty is up to 5 times larger than in the standard case, except in regions where $m_{\nu_e} < 0.2$ eV, as expected from the discussion above. Turning to the output values of the right-handed coupling strength in Fig. 10 we get appallingly bad results, especially in the $m_{\nu_e} = 0.2$ eV region. From the left-hand picture of Fig. 10 one might get the impression that the output value of b is returned rather nicely for the larger masses. However, as shown in the right panel of Fig. 10 the relative error is still up to $\approx 60\%$ in some regions.

In conclusion, we see from these numerical results that it is extremely difficult to get a good determination of *both* the mass and the coupling strength, at least when using fairly large parameter intervals. Given stronger limits the situation would no doubt change, but judging from our COSMOMC contours the values in some cases will be pressed to the largest allowed parameter values, even when the intervals are as broad as here. In other words, tighter parameter values in this case merely amounts to a manual setting of the allowed size of the statistical uncertainties.

Next we perform the analysis on the same spectra without including the right-handed coupling strength to get an idea of the bias imposed on the neutrino mass in the presence of unaccounted-for right-handed currents. We present our results in Fig. 11.

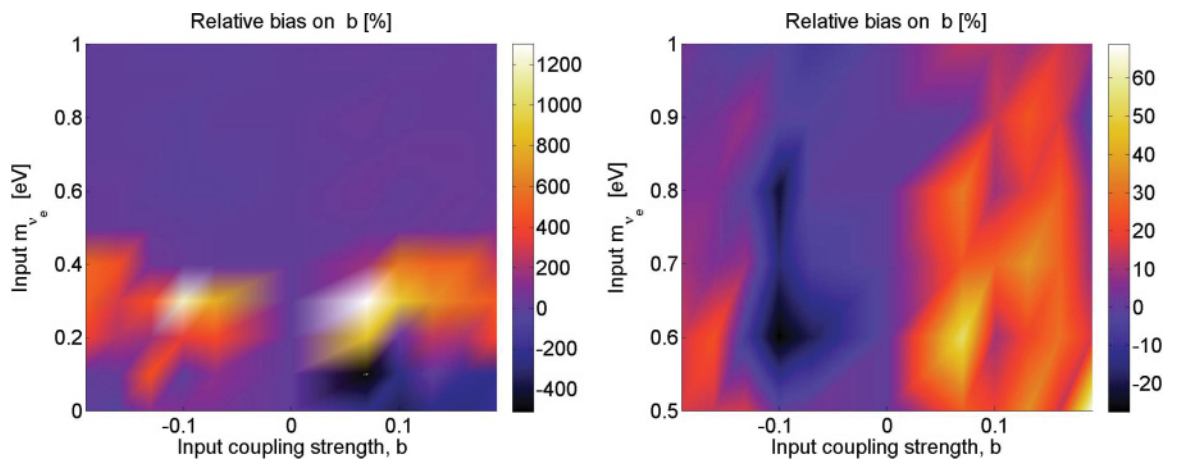


FIG. 10. (Color online) The left figure shows the bias on b for the full parameter range of Table VI and the right figure is an enlarged version of this plot for $m_{\nu_e} > 0.5$ eV. In the left figure we see that we get the output values wrong by more than a factor 10! This is exacerbated at mass values just above the KATRIN's sensitivity, once again demonstrating how the uncertainty on the two ill-determined parameters, m_{ν_e} and b , is redistributed in the parameter space of the Markov chain. The right figure shows us that when we look beyond the much larger error bars around $m_{\nu_e} = 0.2$ eV, the output values still fluctuate with errors of order $\approx 60\%$.

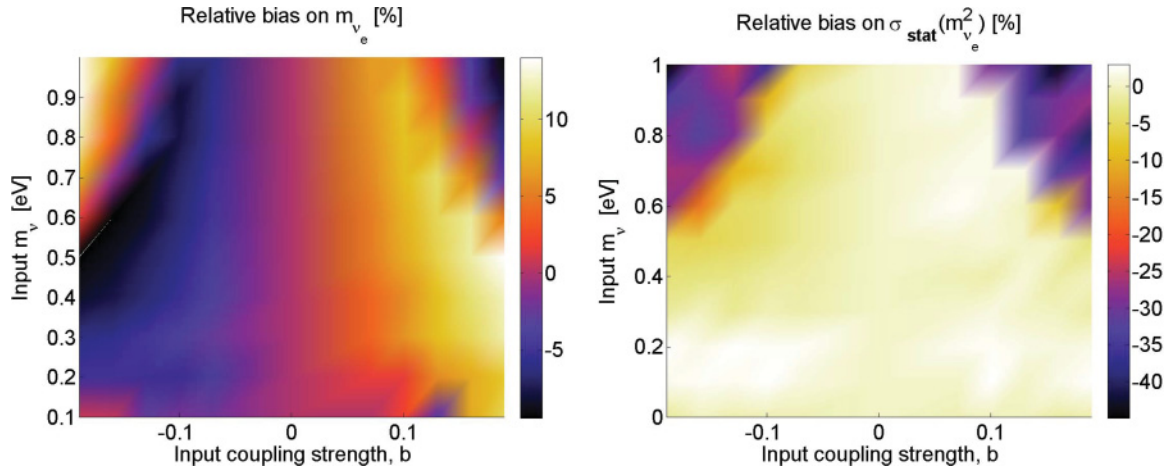


FIG. 11. (Color online) This figure shows the same biases as Fig. 9, but here the analysis has been performed (on the same spectra) without the inclusion of the right-handed coupling strength. Clearly the errors on m_{ν_e} are much better, and for realistic b values, certainly within acceptable $\pm 10\%$ ranges. However, we note that $\sigma_{\text{stat}, m_{\nu_e}^2}$ is $\approx 60\%$ better in the high- b , high- m corners of the right-side plot. This coincides with a turnover of the bias on the mass in the left-side plot. Figure 12 shows that this behavior takes place because the ΔE_0 parameter is being pushed to the maximally allowed values, which should be avoided. That is the uncertainty on the mass due to the presence of b is migrating into the third correlated parameter—the endpoint of the tritium β spectrum.

As it turns out we get much better results when we remove the b dimension from our COSMOMC setup; this time the bias on the mass is no larger than around 12%. We notice, however, that the statistical error drops steeply for high masses and coupling strengths. By inspecting the original COSMOMC likelihood contours we see that this is because ΔE_0 has been pushed to the edge of the input interval as shown in Fig. 12. This also explains why the bias on the mass flips in the same parameter range instead of becoming monotonically larger for maximal coupling strengths. The propagation of the

uncertainty on m_{ν_e} into the ΔE_0 dimension is straightforward from the previously discussed correlations between the b , $m_{\nu_e}^2$, and ΔE_0 parameters. Hopefully the upcoming much more precise ${}^3\text{H}$ – ${}^3\text{He}$ mass measurements [27] will be helpful in resolving this issue for the KATRIN experiment.

The bias induced on the neutrino mass is now within acceptable bounds and agrees well with the results found by Bonn *et al.* [26]. Finally, it should be noted that an experiment such as KATRIN clearly cannot be used to put bounds on the size of the right-handed coupling strength at this point.

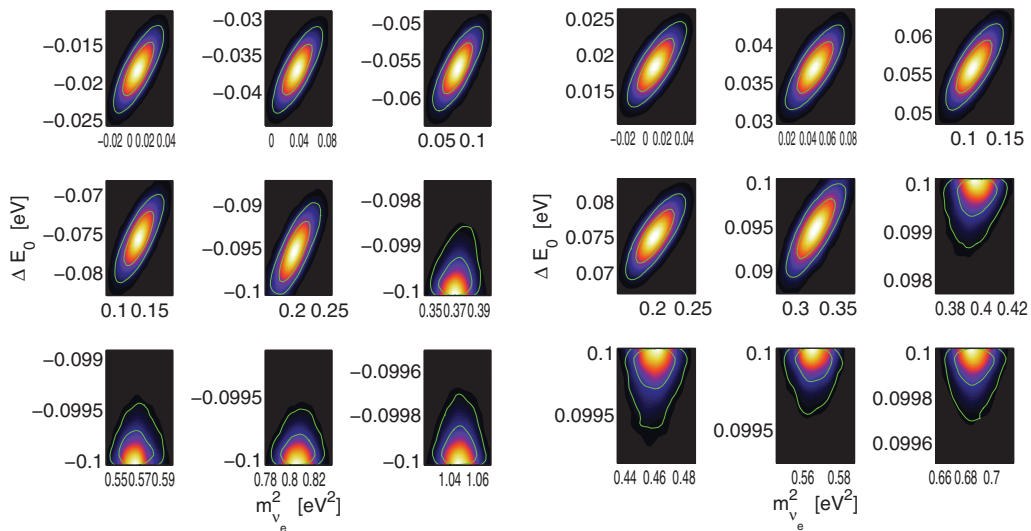


FIG. 12. (Color online) The figure shows the 2D likelihood contours of ΔE_0 vs $m_{\nu_e}^2$ for the mass range 0.1 to 0.9 eV (again going from the upper-left corner to the lower-right corner) when the analysis is performed without the inclusion of b . The figure on the left used spectra that was produced with $b_0 = -0.19$, while the figure on the right is for $b_0 = 0.19$. The expected output for ΔE_0 is zero, but it is clear to see that in this case the b , $m_{\nu_e}^2$, ΔE_0 correlation pushes the uncertainty induced in the mass parameter by the physical presence of b into the ΔE_0 parameter instead.

A precise knowledge of the neutrino mass and the tritium β -spectrum endpoint E_0 would have to be presupposed before measurements of the tritium β spectrum could be used to determine b .

IV. CONCLUSIONS

Our attempt at an analysis of simulated KATRIN data with various additional parameters has shown the following: For the standard case of analysis with regard to one neutrino mass, the MCMC approach is certainly well suited and gives robust results. The method is very practical when performing analysis for nonstandard cases because the COSMOMC output lets us inspect the behavior of the parameters and their relation to one another in a straightforward manner. We have used the method to build a sensitivity plot for a KATRIN-like experiment, clearly demonstrating the dominating dependence of the sensitivity on the signal count rate.

Further, we have learned that for a suitable mass-squared difference an experiment such as KATRIN should be able to detect the existence of other neutrino mass states. And finally, we have re-evaluated the influence of couplings to right-handed currents in the tritium β decay and found that ignoring this would maximally induce an error on the neutrino mass of order 10%.

In conclusion, we find that our Bayesian approach to the analysis of the KATRIN experiment is certainly competitive to a frequentist approach and that it has several advantages when using an already well-developed framework such as COSMOMC.

ACKNOWLEDGMENTS

We acknowledge the use of computing resources from the Danish Center for Scientific Computing (DCSC) and the grant from BMBF under Contract No. 05A08PM1.

-
- [1] A. Osipowicz *et al.* (KATRIN Collaboration), *Progress in Particle and Nuclear Physics* **48**, 141 (2002).
 - [2] J. Angrik *et al.* (KATRIN Collaboration), Wissenschaftliche Berichte FZ Karlsruhe 7090, KATRIN Design Report 2004 (unpublished); [<http://bibliothek.fzk.de/zb/berichte/FZKA7090.pdf>].
 - [3] Ch. Kraus, B. Bornschein, L. Bornschein, J. Bonn, B. Flatt, A. Kovalik, B. Ostrick, E. W. Otten, J. P. Schall, Th. Thümmeler, and Ch. Weinheimer, *Eur. Phys. J. C* **40**, 447 (2005).
 - [4] V. M. Lobashev, *Nucl. Phys. A* **719**, C153 (2003).
 - [5] E. W. Otten and C. Weinheimer, *Rep. Prog. Phys.* **71**, 086201 (2008).
 - [6] K. Nakamura *et al.* (Particle Data Group), *J. Phys. G*, **37**, 075021 (2010).
 - [7] S. S. Masood, S. Nasri, J. Schechter, M. A. Tórtola, J. W. F. Valle, and C. Weinheimer, *Phys. Rev. C* **76**, 045501 (2007).
 - [8] ROOT homepage: [<http://root.cern.ch/drupal>].
 - [9] COSMOMC homepage: [<http://cosmologist.info/cosmomc>].
 - [10] O. Host, O. Lahav, F. B. Abdalla, and K. Eitel, *Phys. Rev. D* **76**, 113005 (2007).
 - [11] J. Hamann, Bayesian Statistics in Cosmology, Danish Astrophysics Research School (DARS); Topics in Cosmology (2008); [http://phys.au.dk/fileadmin/site_files/dars/TiC_Feb08/jan_hamann.pdf].
 - [12] N. Christensen, R. Meyer, L. Knox, and B. Luey, *Classical Quantum Gravity*, **18**, 2677 (2001).
 - [13] L. Perotto, J. Lesgourgues, S. Hannestad, H. Tu, and Y. Y. Y. Wong, *J. Cosmology Astroparticle Physics* **10** (2006) 013.
 - [14] A. Sejersen Riis and S. Hannestad, *J. Cosmology Astroparticle Physics* **02** (2011) 011.
 - [15] Sz. Nagy, T. Fritioff, M. Björkhage, I. Bergström, and R. Schuch, *Europhys. Lett.* **74**, 404 (2006).
 - [16] J. Hamann, S. Hannestad, G. G. Raffelt, and Y. Y. Y. Wong, *J. Cosmology Astroparticle Physics* **08** (2007) 021.
 - [17] E. W. Otten, *Prog. Part. Nucl. Phys.*, **32**, 153 (1994).
 - [18] A. A. Aguilar-Arevalo *et al.* (MiniBooNE Collaboration), *Phys. Rev. Lett.* **98**, 231801 (2007).
 - [19] A. A. Aguilar-Arevalo *et al.* (MiniBooNE Collaboration), *Phys. Rev. Lett.* **105**, 181801 (2010).
 - [20] G. Mention, M. Fechner, Th. Lasserre, Th. A. Mueller, D. Lhuillier, M. Cribier, and A. Letourneau, *Phys. Rev. D* **83**, 073006 (2011).
 - [21] J. Hamann, S. Hannestad, G. G. Raffelt, I. Tamborra, and Y. Y. Y. Wong, *Phys. Rev. Lett.* **105**, 181301 (2010).
 - [22] J. Hamann, S. Hannestad, J. Lesgourgues, C. Rampf, and Y. Y. Y. Wong, *J. Cosmology Astroparticle Physics* **07** (2010) 022.
 - [23] M. C. Gonzalez-Garcia, M. Maltoni, and J. Salvado, *J. High Energy Phys.* **08** (2010) 117.
 - [24] G. J. Stephenson, J. T. Goldman, and B. H. J. McKellar, *Phys. Rev. D* **62**, 093013 (2000).
 - [25] N. Severijns, M. Beck, and O. Naviliat-Cuncic, *Rev. Mod. Phys.* **78**, 991 (2006).
 - [26] J. Bonn, K. Eitel, F. Gluck, D. Sevilla Sanchez, and N. Titov, *Phys. Lett. B* **703**, 310 (2011).
 - [27] K. Blaum, Yu. N. Novikov, and G. Werth, *Contemp. Phys.* **51**, 149 (2010).